https://ntrs.nasa.gov/search.jsp?R=20110008489 2019-08-30T15:00:24+00:00Z

5

The *Swift* Era

Neil Gehrels[1] & David N. Burrows[2]

(1) NASA/Goddard Space Flight Center, Greenbelt, MD 20771, USA
(2) Department of Astronomy and Astrophysics, The Pennsylvania State University, 525 Davey Lab, University Park, PA 16802, USA

5.1 Introduction

The study of gamma-ray bursts (GRBs) remains highly dependent on the capabilities of the observatories that carry out the measurements. The large detector size of BATSE produced an impressively large sample of GRBs for duration and sky distribution studies. The burst localization and repointing capabilities of *BeppoSAX* led to breakthroughs in host and progenitor understanding. The next phase in our understanding of GRBs is being provided by the *Swift* mission. In this chapter we discuss the capabilities and findings of the *Swift* mission and their relevance to our understanding of GRBs. We also examine what is being learned about star formation, supernovae and the early Universe from the new results. In each section of the chapter, we close with a discussion of the new questions and issues raised by the *Swift* findings.

5.2 The *Swift* observatory

Swift (Gehrels et al. 2004) carries 3 instruments: a wide-field Burst Alert Telescope (BAT; Barthelmy et al. 2005a) that detects GRBs and positions them to arcminute accuracy, and the narrow-field X-Ray Telescope (XRT; Burrows et al. 2005a) and UV-Optical Telescope (UVOT; Roming et al. 2005) that observe their afterglows and determine positions to arcsecond accuracy, all within about 2 minutes. BAT is a coded aperture hard X-ray (15–350 keV) imager with 0.5 m^2 of CdZnTe detectors (32,000 individual sensors; ∼2400 cm^2 effective area at 20 keV including mask occultation) and a 1.4 sr half-coded field of view. XRT is a Wolter 1 grazing incidence, imaging X-ray telescope with a 0.2–10 keV energy range, 120 cm^2 effective area at 1.5 keV, field of view of $23'.6 \times 23'.6$, point spread function (PSF) half-power diameter of $18''$ ($7''$ FWHM), and sensitivity of approximately

$2 \times 10^{-14}\,\mathrm{erg\,cm^{-2}\,s^{-1}}$ in 10^4 s. The UVOT is a modified Ritchey-Chrétien reflector with 30 cm aperture, 170–650 nm wavelength range, field of view $17' \times 17'$, PSF FWHM of $1.9''$ at 350 nm, and sensitivity of 23^{rd} magnitude in white light in 10^3 s.

The general operations of the *Swift* observatory are as follows: the BAT detects the bursts in the 15–350 keV band and determines a few-arcminute position onboard, typically within about 20 s. The position is provided to the spacecraft, built by Spectrum Astro (now part of Orbital Sciences Corporation), which repoints to it in less than 2 minutes. The XRT and UVOT then observe the afterglow. Alert data from all three instruments are sent to the ground via NASA's *TDRSS* relay satellite. The full data set is stored and dumped to the Italian Space Agency's equatorial Malindi Ground Station. The *Swift* mission was built by an international team from the US, UK, and Italy, with significant contributions also from Germany and Japan. After five years of development it was launched from Kennedy Space Center on 20 November 2004. The spacecraft and instruments were carefully brought into operational status over an eight week period, followed by a period of calibration and operation verification, which ended with the start of normal operations on 5 April 2005.

Swift started detecting GRBs in December 2004 and was actively following afterglows by February 2005. The mission enables ground-based and other space-based follow-ups of GRBs through rapid data distribution by the GCN network (http://gcn.gsfc.nasa.gov/gcn/). This follow-up complements *Swift* instruments by providing deep optical spectroscopy, IR coverage, rapid response, radio observations, and *HST* and *Chandra* imaging. Recently, new observatories have begun searches for very high energy gamma-rays, neutrinos and gravitational waves in conjunction with *Swift* GRBs. A follow-up team of observers affiliated with *Swift* optimizes use of observatories around the world, representing over 40 telescopes (http://swift.gsfc.nasa.gov/docs/swift/teamlist.html#fu_team).

Swift spends ∼50% of its time observing GRBs and their afterglows, with observations continuing for weeks and even months in some cases. The mission policy is to give highest priority to GRB science. The remaining time is shared between non-GRB planned targets, Target of Opportunity (ToO) observations of non-GRB transients, and calibration sources. All *Swift* science is open to community proposal, through a NASA Guest Investigator program. ToOs can be requested at any time through a public web site, with the decision to observe them made by the *Swift* Principal Investigator based on scientific merit and observational constraints. As of July 2010, more than 2250 ToO requests have been made, and more than 1700 ToO targets have

been observed. Afterglow from 60 GRBs from other observatories has been detected by XRT.

5.3 *Swift* gamma-ray burst observations

As of 1 July 2010, BAT has detected 520 GRBs (annual average rate of about 100 per year). Approximately 80% of the BAT-detected GRBs have repointings within 5 minutes (the remaining 20% have spacecraft constraints that prevent rapid slewing). Of those, virtually all long bursts observed promptly have detected X-ray afterglow, the only exceptions being GRBs 060728, 061027, 070126, and 080315, all of which were marginal detections and possibly not real bursts. Short bursts are more likely to have negligible X-ray afterglow; many have very weak afterglow that fades rapidly below the XRT sensitivity limit, and about 20% (11 out of 54) have no detected X-ray afterglow. The fraction of rapid-pointing GRBs that have a UVOT detection is around 35%. Combined with ground-based optical observations, about 60% of *Swift* GRB have optical afterglow detection.

As of 1 July 2010, there are 167 *Swift* GRBs with redshifts. This total from the first 5.5 years of *Swift* operations is nearly four times the number found from all previous observations since 1997. The distribution in redshift compared to pre-*Swift* measurements is given in Fig. 5.1. It is seen that *Swift* is detecting GRBs at higher redshift than previous missions due to its higher sensitivity and rapid afterglow observations. The average redshift for the *Swift* long GRBs is $\bar{z} = 2.4$ compared to $\bar{z} = 1.2$ for previous observations. Jakobsson et al. (2006a) find that the *Swift* redshift distribution is consistent with models where the GRB rate is proportional to the star formation rate in the Universe.

The duration distribution of *Swift*-detected GRBs is shown in Fig. 5.2. *Swift*'s short- burst fraction is ∼10%, which is smaller than BATSE's ∼25% because *Swift* has a lower energy range than BATSE and short GRBs have hard spectra. Still, the detection rate of short bursts is 10 per year and high enough for considerable progress, as discussed in the following section. Fig. 5.3 shows the duration distribution in the source frame for those bursts with redshift determinations. The typical duration in the source frame is a factor of about 3 less than that in the observer frame, as one would expect from the $(1+z)$ time dilation and average redshift of about 2.4. Long GRBs have true physical durations of typically $10 - 20\,\mathrm{s}$ rather than the $30 - 60\,\mathrm{s}$ that we observe.

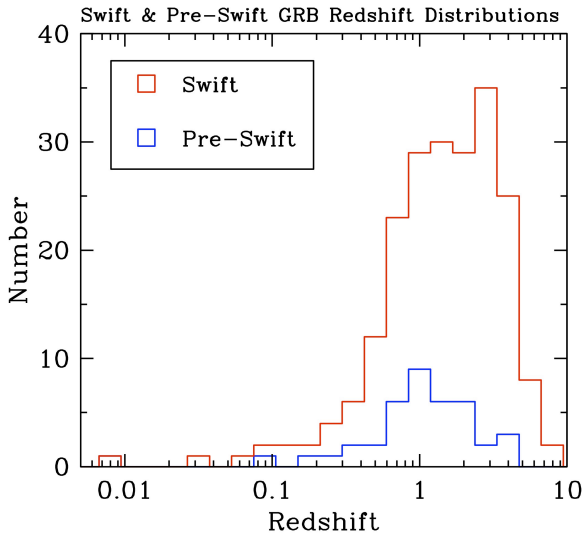

Fig. 5.1. Redshift distribution of *Swift* detected bursts compared to the pre-*Swift* sample.

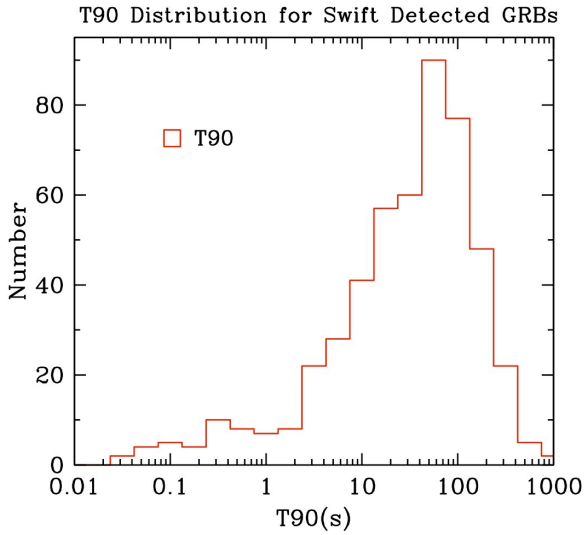

Fig. 5.2. Duration distribution of *Swift* detected bursts. Plotted is the distribution of the parameter T_{90}, which is the length of time in which 90% of the burst fluence is observed.

5.4 Short gamma-ray bursts

At the time of *Swift*'s launch, the greatest mystery of GRB astronomy was the nature of short-duration, hard-spectrum bursts. Although more than 50

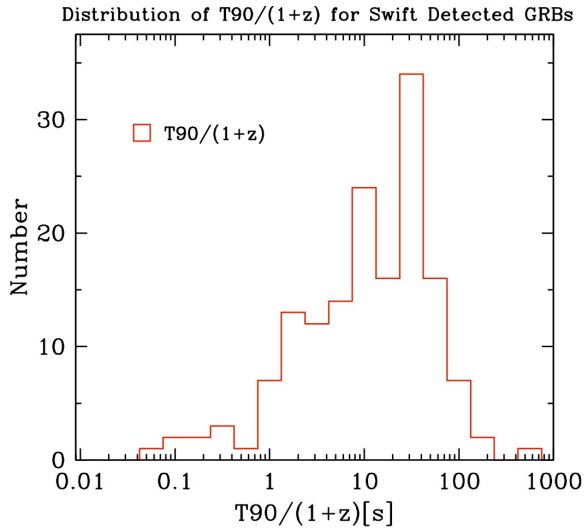

Fig. 5.3. The distribution of durations transposed to the source frame for those *Swift* bursts with redshift determinations.

long GRBs had afterglow detections, no afterglow had been found for any short burst. In May 2005 (GRB 050509B), *Swift* provided the first short GRB X-ray afterglow localization (Gehrels et al. 2005). This burst, plus the *HETE-2* GRB 050709 and *Swift* GRB 050724, led to a breakthrough in our understanding of short bursts (Gehrels et al. 2005, Bloom et al. 2006, Fox et al. 2005, Villasenor et al. 2005, Hjorth et al. 2005, Barthelmy et al. 2005b, Berger et al. 2005). As of 1 July 2010, BAT has detected 54 short GRBs, 80% of which have XRT detections, and 11 of which have firm redshifts. *HETE-2* and *INTEGRAL* have contributed an additional 3 short GRBs with afterglow detections.

In stark contrast to long bursts, the evidence to date on short bursts is that they typically originate in host galaxies with a wide range of star formation properties, though within these galaxies they seem to occur in regions with low star formation rate. GRB 050509B and 050724 were from elliptical galaxies with low current star formation rates, while GRB 050709 was from a region of a star forming galaxy with no nebulosity or evidence of recent star formation activity in that location. This is illustrated in Fig. 5.4, where the images of these 3 short bursts are contrasted to 3 typical *HST* images of long bursts, which are typically coincident with regions of star formation (Fruchter et al. 2006). Taken together, these results support the interpretation that the progenitors of short bursts have a broad distribution of time delays between stellar birth and explosive death, and may arise from

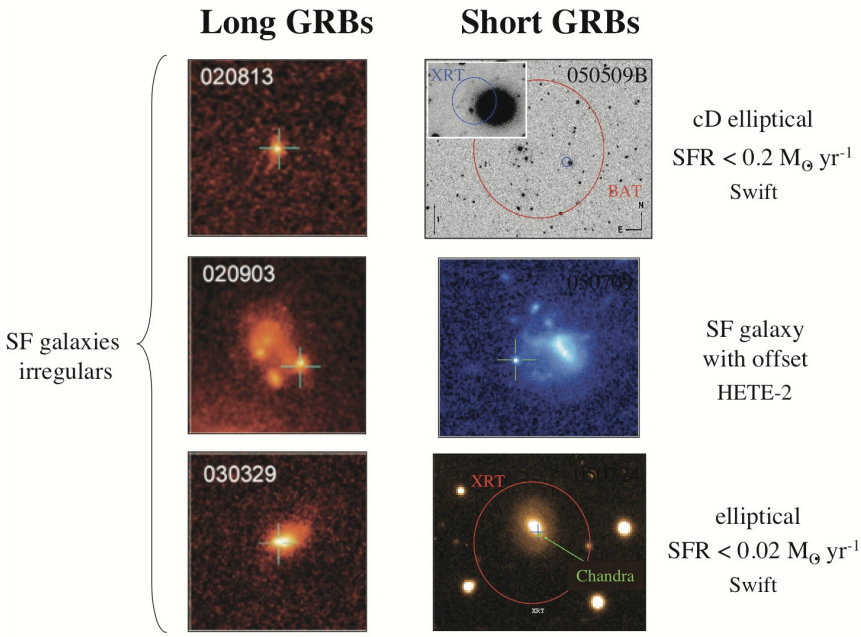

Fig. 5.4. Images of 3 short GRBs compared to 3 typical long GRBs. The short GRBs and image references are GRB 050509B (Gehrels et al. 2005), GRB 050709 (Fox et al. 2005) and GRB 050724 (Barthelmy et al. 2005b). The long burst images are from Fruchter et al. (2006).

mergers of compact binaries (i.e., double neutron star or neutron star - black hole (NS-BH) binaries).

In Fig. 5.5 we show the redshift distribution of *Swift* short bursts compared with long bursts. Only GRBs with firm redshifts were included. With the caveat that statistics are poor and the population appears diverse, the redshifts for short bursts are smaller on average by a factor of ~ 4 than those of long bursts ($\bar{z}_{\rm short} = 0.5$, $\bar{z}_{\rm long} = 2.4$).

Measurements or constraining limits on beaming from light curve break searches have been hard to come by with the typically weak afterglow of short GRBs. In Fig. 5.6 (from Burrows et al. 2006) we compare the inferred beaming angle distributions for long and short GRBs. Given the uncertainties associated with small number statistics, the distribution of beaming angles for short GRBs appears to be broad and roughly consistent with that for long GRBs. Further observations of short GRB jet breaks are needed to make firm conclusions.

Swift observations also reveal new and puzzling features. Long ($\sim$100 s) 'tails' with softer spectra than the first episode follow the prompt emission

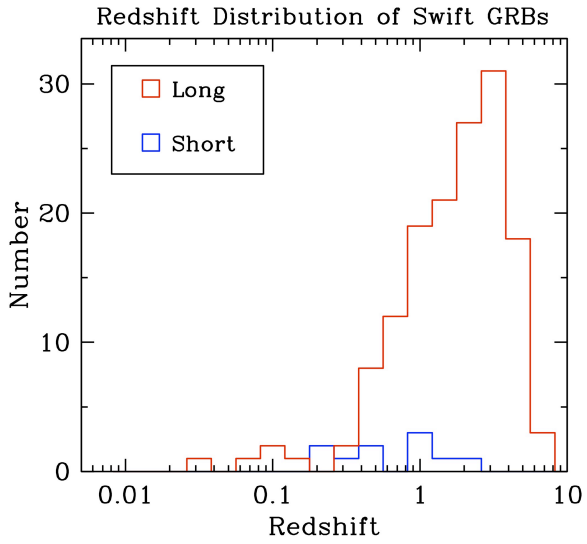

Fig. 5.5. Redshift distribution of *Swift* short and long GRBs.

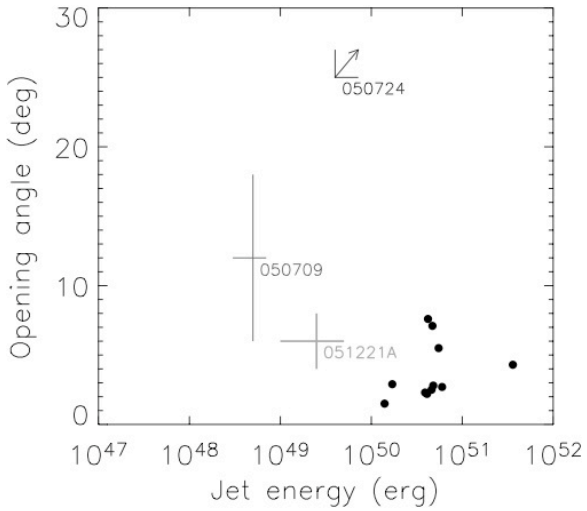

Fig. 5.6. Jet opening angles for short and long GRBs as estimated from observations of jet breaks in the light curves. The black points are typical long bursts (from Burrows et al. 2006).

for about 25% of short bursts (Norris & Bonnell 2006, Gehrels et al. 2006). Also, X-ray flares on late timescales in the afterglow (Barthelmy et al. 2005b, Campana et al. 2006a) are not easily explained by the standard coalescence model. Perhaps these flares result from a complex energy extraction process

from the nascent black hole, or self-gravitational clumping instabilities at large radii in the fall-back disk (Perna et al. 2006), or other possibilities (MacFadyen et al. 2005, Rosswog 2007, Lee et al. 2007, Metzger et al. 2010).

Swift localization of a short GRB increases the sensitivity of gravitational-wave interferometers to detect gravitational waves from that GRB by a large factor due to the much narrower search window that can be used (Finn et al. 1999). Detection of gravitational waves from a *Swift* GRB would be an enormous discovery with great scientific payoff for merger physics, progenitor types, and NS equations of state. Short GRBs are also 'cosmic sirens' that can provide constraints on the properties of dark energy, if they are detected by gravitational-wave detectors (Dalal et al. 2006). While LIGO has not yet detected the gravitational-wave signature of any short GRB, it is expected that the Advanced LIGO, which will become operational in 2015, will be sensitive enough to detect short GRBs; it is feasible for *Swift* to be operating at that time, and the combination of *Swift* and Advanced LIGO will provide a powerful tool to confirm theoretical predictions of NS merger events.

We already know from the 27 December 2004 extremely luminous giant flare from SGR 1806–20 that such events could be detected to ∼60 Mpc and would look identical to short GRBs (Palmer et al. 2005). With *Swift*, we can determine whether some short GRBs are magnetar flares or whether the SGR 1806–20 giant flare was an extremely rare event. A study (Nakar et al. 2006) that searched for nearby galaxies ($z < 0.025$) within the error boxes of six well-localized, pre-*Swift* short GRBs failed to find any plausible hosts, as would be expected from magnetar progenitors, and concludes that magnetar hyperflares constitute <15% of all short GRBs. The detection of the short, intense burst GRB 070102 by IPN (Mazets et al. 2008), with an error box that overlapped an arm of the Andromeda galaxy (M31), may have been such an extragalactic magnetar flare. No LIGO merger signal was seen for this burst (Abbott et al. 2008), confirming that it was not due to a NS-NS merger in M31. The only question for the magnetar interpretation is whether the burst actually was located in the Andromeda galaxy, given the large size (446 square arcminutes) of the error box.

5.4.1 Short gamma-ray burst open questions

Although a huge step forward has been accomplished with the short burst observations over the past 5 years, the origin and nature of short GRB is far from settled. The following are questions that have been raised by the new data:

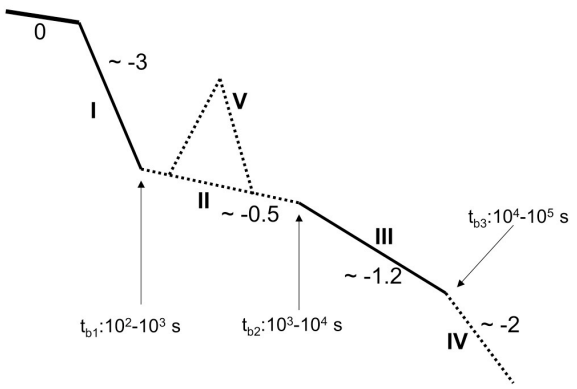

Fig. 5.7. Schematic of the log flux-log time relation of various X-ray afterglow phases seen in GRBs (taken from Zhang et al. 2006). The prompt phase (0) is often followed by a steep decline afterglow (I) which can then break to a shallower decline (II), a standard afterglow phase (III), and possibly, a jet break (IV). Flares (V) can be superimposed on any segment, but are most commonly seen in the early afterglow (phases I and II).

(i) Are short bursts caused by merging neutron stars or some other mechanism associated with old stellar populations with a wide range of time delays between stellar birth and explosion?
(ii) What is the distance distribution of short GRBs? The distance range of short bursts extends from $z = 0.2$ to $z = 1$ and possibly $z = 2.6$ (GRB 090426); the distance range is wide (Berger et al. 2007).
(iii) What is the distribution of beaming angles for short GRBs? There are few good data on jet opening angles to date.
(iv) What is the origin of the long soft tails seen on 25% of short GRBs?

5.5 Afterglow physics

Swift was specifically designed to investigate GRB afterglows by filling the temporal gap between observations of the prompt emission and the later, fading afterglow (O'Brien et al. 2006a). The combined power of the BAT and XRT has revealed that in long GRBs the prompt X-ray emission smoothly transitions into the decaying afterglow (Fig. 5.7 & 5.8). Often, a steep-to-shallow transition (phases I – II in Fig. 5.7) is found, suggesting that prompt emission and the afterglow are distinct emission components. This also seems to be the case for short bursts (Burrows et al. 2006).

The early steep-decay phase seen in the majority of GRBs was a real surprise. The current best explanation is that we are seeing high-latitude emis-

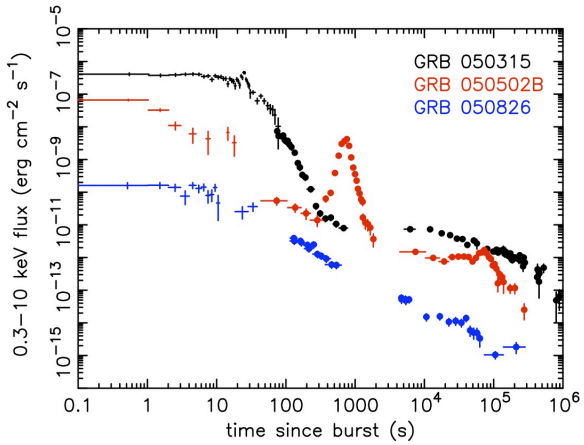

Fig. 5.8. Example GRBs with steep-to-shallow transition (GRB 050315), large X-ray flare (GRB 050502B) and more gradually declining afterglow (GRB 050826; flux scale divided by 100 for clarity). Figure from O'Brien et al. (2006b).

sion due to termination of central-engine activity (Barthelmy et al. 2005c, Kumar & Panaitescu 2000, Zhang et al. 2006). This phase is usually followed by an equally unexpected shallow decay phase (the plateau phase) that begins within the first hour. The plateau phase can last for up to a day, and, although faint, is energetically very significant. It is likely due to the forward shock being constantly refreshed (Zhang et al. 2006, Rees & Mészáros 1998, Nousek et al. 2006) by either late central engine activity or less relativistic material emitted during the prompt phase. Alternatively, Granot et al. (2006) show how the flat decay phase can be explained by a two-component jet model (Peng et al. 2005) in which a narrow, initially highly relativistic, conical jet (producing the prompt emission) is embedded within a mildly relativistic coaxial cone that decelerates markedly as it plows into the CSM.

The transition between the steeply decaying initial phase and the plateau phase can provide information on the radius at which the prompt emission is generated. Studies of a small sample of bursts with cleanly defined transitions shows that the prompt emission from some bursts cannot be produced in internal shocks, and suggests that the outflow might be magnetic rather than particle-dominated (Kumar et al. 2007).

In Fig. 5.9 we show a sample of bright *Swift* UVOT optical light curves (Oates et al. 2009). Most *Swift*-localized GRBs are optically faint at early times (Roming et al. 2006), in contrast to some pre-*Swift* expectations, and there is little evidence for bright optical emission from reverse shocks. Un-

like the X-ray afterglows, a substantial fraction of optical afterglows begin with a slow rise representing the afterglow onset (Fig. 9); this phase is generally obscured in X-ray afterglows by the bright tail of the prompt emission (Willingale et al. 2007). In most GRBs, the optical afterglow decays from the beginning of the observation as $t^{-1.5}$ or shallower, with the brighter optical afterglows decaying more steeply on average than the fainter ones (Oates et al. 2009). Here, the afterglow emission may be dominated by the external shock, as expected prior to *Swift* (phase III in Fig. 5.7). In this case, one expects the optical and X-ray afterglows to track one another, as is seen in GRB 050801 (Rykoff et al. 2006). However, a surprisingly large fraction of bursts with strong optical and X-ray afterglow behave in ways that seem contrary to the expectations of the standard fireball model for afterglows, with optical breaks that are unaccompanied by X-ray breaks, X-ray breaks unaccompanied by optical breaks, or with slopes that cannot be mutually reconciled with model expectations (Panaitescu et al. 2006). A notable example was the ultra-bright GRB 080319B, the so-called 'naked-eye' burst, with particularly bright, well-studied optical and X-ray afterglow light curves that cannot be reconciled to the standard models without assumption of multiple components from a structured jet (Racusin et al. 2008).

Swift has found erratic flaring behavior in X-ray afterglow (phase V in Fig. 5.7), lasting long after the prompt phase, in some cases for several hours after the burst. The most extreme examples are flares with integrated power comparable to the initial burst (Burrows et al. 2005b, Falcone et al. 2006). The rapid rise and decay, multiple flares in the same burst, and cases of fluence comparable with the prompt emission suggest that these flares are due to continuing activity of the central engine (Burrows et al. 2007).

There is a lack of evidence for jet breaks (breaks in temporal decay slope, phase III — IV transition in Fig. 5.7) in the *Swift* X-ray afterglow (Willingale et al. 2007, Sato et al. 2007, Burrows & Racusin 2006, Kocevski & Butler 2008, Liang et al. 2008). Although possible jet breaks have been measured in some bursts, the number of bursts in which clear jet breaks are seen is small and they often do not satisfy the empirical relations previously found from optical observations (Frail et al. 2001, Bloom et al. 2003, Liang et al. 2008). A rare example of a near-textbook achromatic jet break in both X-ray and optical bands is seen in GRB 060526 at redshift $z = 3.21$ (Fig. 5.10), where the late-time optical and X-ray afterglows are consistent with a break at about T_0+240 ks, consistent with an opening angle of $\theta_{\rm j} \sim 7^\circ$ (Dai et al. 2007). GRB 060614 presents another nearly textbook example (Mangano et al. 2007), with an achromatic jet break at about 117 ks and an opening angle of about 9°, but there are very few of these. One possibility

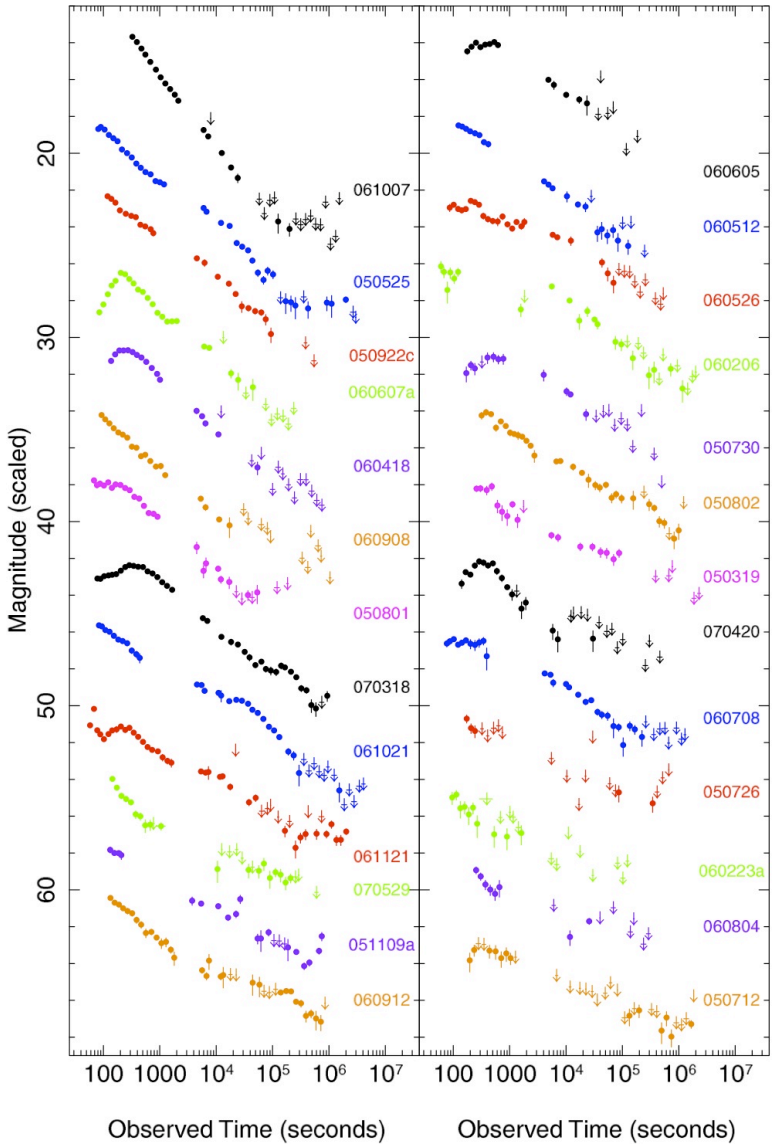

Fig. 5.9. *Swift* UVOT light curves for a sample of bursts, ordered by decreasing peak magnitude from the brightest (GRB 061007) to the faintest (GRB 050712), with arbitrary offsets for display purposes. Arrows indicate 3σ upper limits (from Oates et al. 2009).

for the paucity of observed jet breaks is that they are occurring at later times in the *Swift* sample due to the higher redshifts of these bursts, but this seems insufficient to resolve the apparent discrepancies with previous

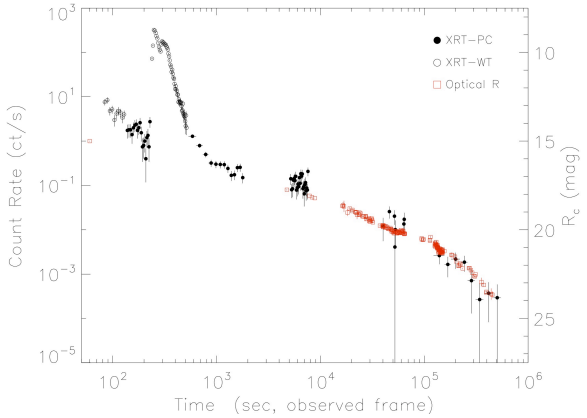

Fig. 5.10. XRT (black) and R band (red) observations of GRB 060526, from Dai et al. (2007). This is a rare example of a near-textbook jet break in the optical and X-ray bands, with both bands breaking to the same slope at the same time ($\sim 2.4 \times 10^5$ s).

results (Burrows & Racusin 2006, Kocevski & Butler 2008). It is more likely that jet breaks are often either hidden in the late-time light curves (Curran et al. 2008) or are missed due to confusion with other portions of the complex X-ray light curves (Racusin et al. 2009).

5.5.1 Afterglow physics open questions

The early X-ray and optical afterglow observations obtained by *Swift* had provided new insights into the central engine of GRBs and seem generally consistent with the fireball model of their afterglows, but have opened the following new questions:

(i) Why do we not see the same kind of jet behavior in *Swift* bursts that was inferred from pre-*Swift* observations?
(ii) Is there really a common energy reservoir in GRBs, as suggested by earlier, primarily optical afterglows?
(iii) What produces the plateau phase in the X-ray afterglows? Is it caused by energy injection into the external shock, by continuation of central engine activity and internal shocks, by more complex jet structure, or by other mechanisms?
(iv) Is the outflow from the central engine dominated by particles or is it electromagnetic?
(v) How can we explain the frequent discrepancies between the optical and X-ray afterglows?

5.6 Lack of spectral lines in prompt and afterglow emission

Pre-*Swift* claims of the detection of cyclotron lines in GRB prompt emission raised the possibility that GRBs originated in highly magnetized neutron stars (Yoshida et al. 1991, Murakami 1991, Isenberg et al. 1998, and references therein), suggesting that the improved sensitivity and spectral resolution of the *Swift* BAT would provide important constraints on GRB progenitors. However, no lines have been found in BAT spectra of GRB prompt emission, which are always found to be consistent with either power law, cutoff power law, or Band function continuum models. Other, less direct arguments based on characteristics of some X-ray afterglows have suggested that magnetars may exist, at least briefly, in some GRBs (Troja et al. 2007, Lyons et al. 2010, Rowlinson et al. 2010), but there has been no direct confirmation by detection of cyclotron lines in *Swift* data.

Similarly, pre-*Swift* reports of the detection of Fe K emission lines (Antonelli et al. 2000, Piro et al. 1999, 2000, Yoshida et al. 1999) and absorption edges (Amati et al. 2000, Frontera et al. 2004) and lines of other elements (Reeves et al. 2002, Watson et al. 2002, 2003) in X-ray afterglows suggested that early, sensitive observations with good energy resolution would allow determination of GRB redshifts and environments based directly on X-ray afterglow spectra. However, the methods used in many of these reports have been criticized as over-estimating the statistical significance of the reported features (Sato et al. 2005). Early afterglow observations by the *Swift* XRT have found no evidence for emission lines from GRBs (Hurkett et al. 2008), and no deep observations by XMM-Newton and Suzaku have detected emission lines from GRBs since *Swift* was launched. X-ray afterglow spectra are invariably consistent with continuum spectra: power laws in most cases, with a few instances of thermal components for GRBs associated with nearby supernovae (Campana et al. 2006b, Starling et al. 2010; see Section 5.8.1), and with some cutoff power laws during bright X-ray flares (Falcone et al. 2006).

5.7 High-redshift gamma-ray bursts and cosmology

GRBs, as the most brilliant explosions we know of, offer the potential to probe the early Universe into the epoch of reionization. They can trace the star formation, re-ionization, and metallicity histories of the Universe (Lamb & Reichart 2000, Lamb 2002, Ciardi & Loeb 2000, Bromm & Loeb 2002). GRBs are 100–1000 times brighter at early times than are high-redshift QSOs (the near infrared afterglow of GRB 050904 was $J = 17.6$ at 3.5 h). Furthermore, they are expected to occur out to $z > 10$, whereas QSOs

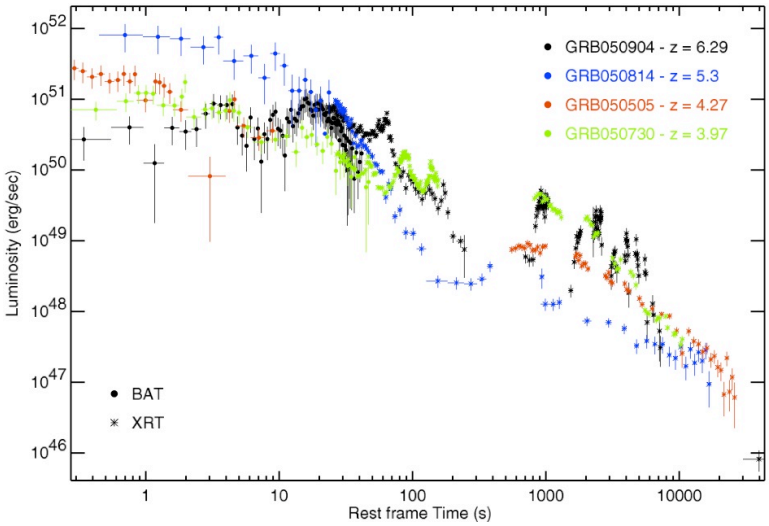

Fig. 5.11. Light curves (BAT-XRT) of 4 high-z *Swift* bursts (from Cusumano et al. (2007).

drop off beyond $z = 3$. Another benefit is that GRB afterglows produce no 'proximity effects' on intergalactic distances scales, and have simple power-law spectra and no emission lines. Thus GRBs are 'clean' probes of the intergalactic medium (IGM).

The 10 highest-redshift GRBs ever seen were discovered by *Swift* (Fig. 5.1), including bursts at redshifts $z = 5.3$ (Jakobsson et al. 2006b), 5.6 (Haislip et al. 2006), 6.3 (Kawai et al. 2006), 6.7 (Ruiz-Velasco et al. 2007), and 8.2 (Greiner et al. 2009, Tanvir et al. 2009, Salvaterra et al. 2009, Chandra et al. 2010). Of the GRBs with measured redshift, we find that only 5 out of 167 bursts with redshift, or about 3% of *Swift* GRBs, lie at $z > 5$, which is much lower than pre-*Swift* predictions (Bromm & Loeb 2002). Nevertheless, these same models predict that *Swift* can detect GRBs to redshifts of $z > 8$, and a great deal of effort is currently being invested to rapidly recognize such bursts and obtain redshifts with large ground-based IR spectrographs. The time evolution of gamma-ray and X-ray fluxes of 4 high-redshift GRBs is shown in Fig 5.11. All of these bursts are quite luminous and long-lasting, and their evolution can be very complex.

Swift's rapid localizations have provided new opportunities for spectroscopy of high-redshift GRB afterglows. Observed at low resolution, the host galaxy appears as a damped Ly-α (DLA) system along with a rich array of metallic lines which can be used to infer metal abundances. At high resolution, the host absorption lines split into an array of fine-structure transitions, which

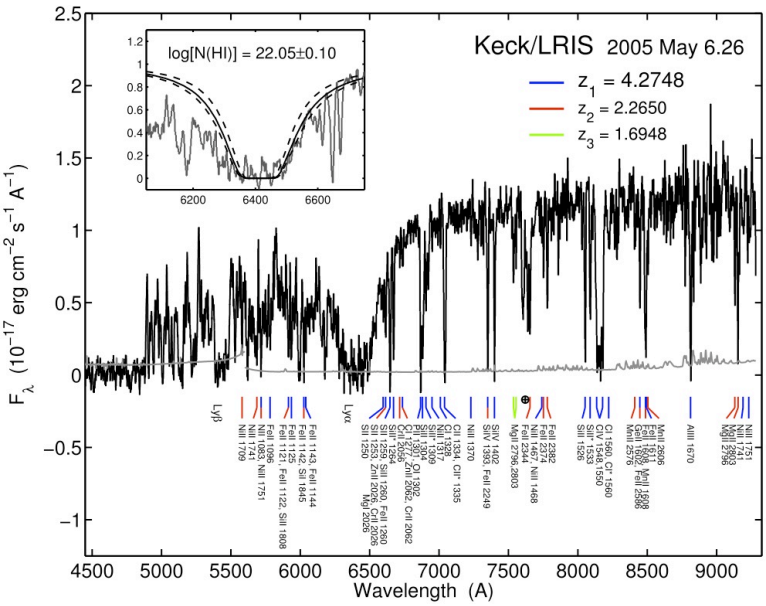

Fig. 5.12. GRB 050505 optical spectrum. Lines are seen from the host galaxy at z=4.275 as well as two foreground absorbers. Figure from Berger et al. (2006).

allows the inference of gas densities and even of diffuse radiative conditions in the host galaxy (Chen et al. 2005, Berger et al. 2006). Fig. 5.12 is an example of an optical spectrum for a high-redshift ($z = 4.3$) GRB (Berger et al. 2006). Countless lines are evident in the spectrum, including a damped Ly-α feature corresponding to a neutral hydrogen column density of $10^{22}\,\mathrm{cm}^{-2}$. The lines imply a density of $100\,\mathrm{cm}^{-3}$ in the source region. Absorption lines observed in infrared spectroscopic observations of GRB 050904 gave a metallicity measurement of 5% solar (Kawai et al. 2006), the first metallicity determination at such high redshift, demonstrating that the observed evolution in the mass- and luminosity- metallicity relationships from $z = 0$ to 2 continues to $z > 6$ (Berger et al. 2006).

5.7.1 High-redshift gamm-ray burst open questions

The detections of GRB 050904 at $z = 6.29$ and 16 other bursts with the very high redshifts of $z > 4$, including GRB 090423 at $z = 8.2$, have opened up a new area of study of the high-redshift Universe. Deep spectroscopic observations with large telescopes are providing measurements of stellar and galactic properties such as metallicity that are not available by other means. Future progress is needed to answer the following open questions:

(i) Is the GRB rate proportional to the star formation in the Universe to high redshift?

(ii) What is the metallicity history of the Universe?

(iii) When did reionization occur in cosmic history?

(iv) Do the explosions of Pop III stars create GRBs?

5.8 Probing the gamma-ray burst-supernova connection

5.8.1 Supernova shock breakout in GRB 060218 and GRB 100316D

On 18 February 2006 *Swift* detected the remarkable burst GRB 060218 (Campana et al. 2006b), which provided considerable new information on the connection between SNe and GRBs. It lasted longer and was softer than any previous *Swift* burst, and was associated with SN 2006aj at only $z = 0.033$. The BAT trigger enabled XRT and UVOT observations during the prompt phase of the GRB and initiated multiwavelength observations of the supernova starting at the time of the initial core collapse. The spectral peak in prompt emission at ∼5 keV places GRB 060218 in the X-Ray Flash (XRF; Heise et al. 2001) category of GRBs (Campana et al. 2006b). Combined BAT-XRT-UVOT observations provided the first direct observation of shock-breakout in a SN (Campana et al. 2006b, Waxman et al. 2007). This is inferred from the evolution of a soft thermal component in the X-ray and UV spectra, and early- time luminosity variations. The associated supernova, SN 2006aj, was dimmer by a factor of about 2 than the previous SNe associated with GRBs, but still 2–3 times brighter than normal SNe Ic not associated with GRBs (Pian et al. 2006, Mazzali et al. 2006).

GRB 100316D was a remarkably similar event: an XRF with an unusually long ($T_{90} > 1300$ s), soft prompt emission phase that allowed XRT and UVOT observations during the prompt phase (Starling et al. 2010). The GRB was associated with SN 2010bh in a nearby galaxy at $z = 0.059$. The early X-ray light curve was flat and smooth and was spectrally consistent with the sum of a power law and a blackbody thermal spectrum.

GRB 060218 and GRB 100316D were underluminous bursts, as were 2 of the other 3 previous GRBs associated with SNe (e.g., Kaneko et al. 2007) Because of the low luminosity, these events are only detected when nearby and are therefore rare occurrences. However, they are actually some 10 times more common in the Universe than normal GRBs (Soderberg et al. 2006).

5.8.2 The peculiar case of GRB 060614

GRB 060614 was a low-redshift, long-duration burst with no detection of a coincident supernova to deep limits. It was a bright burst (fluence in $15-150\,\mathrm{keV}$ band of $2.2\times10^{-5}\,\mathrm{erg\,cm^{-2}}$) and was well studied in the X-ray and optical (Mangano et al. 2007). With a T_{90} duration of 102 s, it seemingly falls squarely in the long burst category. A host galaxy was found (Gal-Yam et al. 2006, Fynbo et al. 2006, Della Valle et al. 2006) at $z=0.125$ and deep searches were made for a coincident supernova. Almost all other well-observed nearby GRBs have had supernovae detected, but this one did not to limits more than 100 times fainter than previous detections (Gal-Yam et al. 2006, Fynbo et al. 2006, Della Valle et al. 2006).

We have found that GRB 060614 shares some characteristics with short bursts (Gehrels et al. 2006). The BAT light curve (see Fig. 5.13) shows a first short, hard-spectrum episode of emission (lasting 5 s) followed by an extended and somewhat softer episode (lasting ∼100 s). The total energy content of the second episode is five times that of the first [fluence of $(1.69\pm0.02)\times10^{-5}\,\mathrm{erg\,cm^{-2}}$ and $(3.3\pm0.1)\times10^{-6}\,\mathrm{erg\,cm^{-2}}$, respectively, in the 15–350 keV band]. The light curve appearance (short hard episode followed by long soft emission) is similar in many respects to that of several recent *Swift* and *HETE-2* short-duration bursts and a subclass of BATSE short bursts (Norris & Bonnell 2006). There are differences in that the short episode of this burst is longer than the previous examples and the soft episode is relatively brighter and more variable. Another similarity with short bursts comes from a lag analysis of GRB 060614 (Gehrels et al. 2006). The lag for GRB 060614 for the first 5 s is 3 ± 6 ms, which falls in the same region of the lag-luminosity plot as short bursts.

It is difficult to determine unambiguously which category of burst the well-observed GRB060614 falls into. It is a long event by the traditional definition, but it lacks an associated SN as had been seen in nearly all other nearby long GRBs. It shares some similarities with *Swift* short bursts, but has important differences such as the brightness of the extended soft episode. If it is due to a collapsar, it indicates that some massive star collapses either fail as supernovae or highly underproduce ^{56}Ni. If it is due to a merger, then the bright long-lived soft episode, brighter relative to the short pulse than for any other soft episode, is hard to explain for a clean NS-NS merger, where little accretion is expected at late times (but might fit in a NS-BH scenario). In any case, this peculiar burst is challenging our classifications of GRBs (Gehrels et al. 2006, Zhang et al. 2007, 2009).

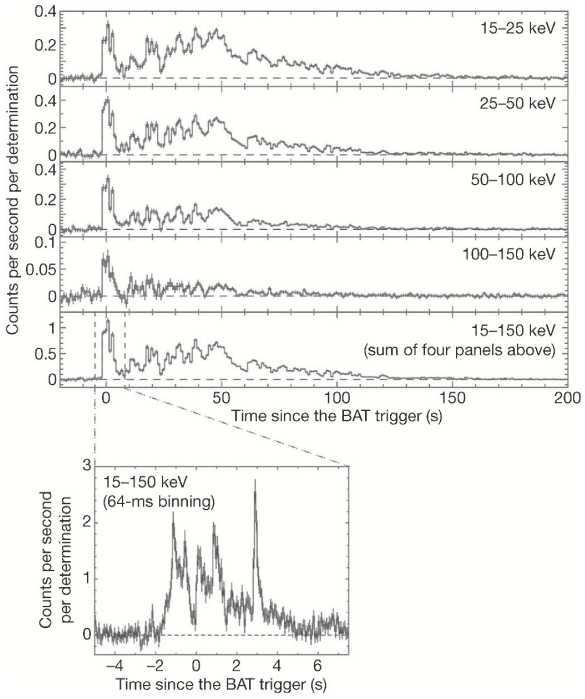

Fig. 5.13. The light curve of the prompt emission of GRB 060614 as measured by the BAT. The light curve is shown in four energy channels plus a sum. The first 5 s of the burst is shown in detail at the bottom (from Gehrels et al. 2006).

5.8.3 Gamma-ray burst-supernova connection open questions

Although the average redshift of *Swift* bursts is large, there are still a good number of events detected at small enough distance for sensitive supernova searches. During its expected 10 year mission lifetime *Swift* will detect about 10 nearby ($z < 0.1$) GRBs. With these data, the following open questions can be addressed:

(i) Are all GRBs accompanied by SNe?

(ii) What is the rate of underluminous GRBs per unit volume in the local Universe and how does it compare to the rate of normal GRBs?

(iii) What is the physical origin of bursts like GRB 060614, which have long durations and low limits on the brightness of any possible coincident supernova?

5.9 Conclusions

The study of GRBs has advanced greatly since the launch of *Swift* in late 2004. *Swift* is providing rapid and accurate localizations, which lead to intensive observing campaigns by *Swift* and ground-based observatories starting within minutes after the GRB trigger. Uniform multiwavelength afterglow light curves are available for the first time for a large number of bursts. The data have led to a break-through in our understanding of short GRBs, have extended our knowledge of the high-redshift Universe, have elucidated the physics taking place in the highly relativistic GRB fireball outflows and have added significantly to the study of the connection between GRBs and SNe. The *Swift* mission has an orbital lifetime of over 10 years and no expendable resources on board, and so is likely to greatly expand on these results with detailed observations of more than 1000 bursts.

Acknowledgements: We acknowledge the contributions of members of the *Swift* science team in producing the figures and data in this chapter. Contributions of particular importance to this work were made by J.D. Myers.

References

Abbott, B., et al. (2008). *ApJ* **681**, 1419.
Amati, L., et al. (2000). *Science* **290**, 953.
Antonelli, L.A., et al. (2000). *ApJ* **545**, L39.
Barthelmy, S.D., et al. (2005a). *Space Sci. Rev.* **120**, 143.
Barthelmy, S.D. et al. (2005b). *Nat* **438**, 994.
Barthelmy, S.D., et al. (2005c). *ApJ* **635**, L133.
Berger, E., et al. (2005). *Nat* **438**, 988.
Berger, E., et al. (2006). *ApJ* **642**, 979.
Berger, E. et al. (2007). *ApJ* **664**, 1000.
Bloom, J.S., Frail, D.A., & Kulkarni, S.R. (2003). *ApJ* **594**, 674.
Bloom, J.S., et al. (2006). *ApJ* **638**, 354.
Bromm, V. & Loeb, A. (2002). *ApJ* **575**, 111.
Burrows, D.N., et al. (2005a). *Space Sci. Rev.* **120**, 165.
Burrows, D.N., et al. (2005b). *Science* **309**, 1833.
Burrows, D.N. & Racusin, J. (2006). *Nuovo Cim. B* **121**, 1273.
Burrows, D.N., et al. (2006). *ApJ* **653**, 468.
Burrows, D.N., et al. (2007). *Phil. Trans. of the R. Soc. A* **365**, 1213.
Campana, S., et al. (2006a). *A&A* **454**, 113.
Campana, S., et al. (2006b). *Nat* **442**, 1008.
Chandra, P., et al. (2010). *ApJ* **712**, L31.
Chen, H.-W., Prochaska, J.X., Bloom, J.S., & Thompson, I.B. (2005). *ApJ* **634**, L25.
Ciardi, B. & Loeb, A. (2000). *ApJ* **540**, 687.
Curran, P.A., van der Horst, A.J., & Wijers, R.A.M.J. (2008). *MNRAS* **386**, 859.
Cusumano, G., et al. (2007). *A&A* **462**, 73.

Dai, X., et al. (2007). *ApJ* **658**, 509.
Dalal, N., Holz, D.E., Hughes, S.A., & Jain, B. (2006). *Phys. Rev. D* **74**, 063006.
Della Valle, M., et al. (2006). *Nat* **444**, 1050.
Falcone, A., et al. (2006). *ApJ* **641**, 1010.
Finn, L.S., Mohanty, S.D., & Romano, J.D. (1999). *Phys. Rev. D* **60**, 121101.
Fox, D.B., et al. (2005). *Nat* **437**, 845.
Frail, D.A., et al. (2001). *ApJ* **562**, L55.
Frontera, F., et al. (2004). *ApJ* **616**, 1078.
Fruchter, A.S., et al. (2006). *Nat* **441**, 463.
Fynbo, J.P.U., et al. (2006). *Nat* **444**, 1047.
Gal-Yam, A., et al. (2006). *Nat* **444**, 1053.
Gehrels, N., et al. (2004). *ApJ* **611**, 1005.
Gehrels, N., et al. (2005). *Nat* **437**, 851.
Gehrels, N., et al. (2006). *Nat* **444**, 1044.
Granot, J., Königl, A., & Piran, T. (2006). *MNRAS* **370**, 1946.
Greiner, J., et al. (2009). *ApJ* **693**, 1610.
Haislip, J., et al. (2006). *Nat* **440**, 181.
Heise, J., in 't Zand, J.J.M., Kippen, R.M., & Woods, P.M. (2001). in Gamma-Ray Bursts in the Afterglow Era, eds. E. Costa, F. Frontera, & J. Hjorth (Berlin:Springer), p. 16.
Hjorth, J. et al. (2005). *Nat* **437**, 859.
Hurkett, C.P., et al. (2008). *ApJ* **679**, 587.
Isenberg, M., Lamb, D.Q. & Wang, J.C.L. (1998). *ApJ* **493**, 154.
Jakobsson, P., et al. (2006a). in Gamma-Ray Bursts in the *Swift* Era, eds. S.S. Holt, N. Gehrels & J.A. Nousek (New York: AIP), p. 552.
Jakobsson, P., et al. (2006b). *A&A* **447**, 897.
Kaneko, Y., et al. (2007). *ApJ* **654**, 385.
Kawai, N., et al. (2006). *Nat* **440**, 184.
Kocevski, D. & Butler, N. (2008). *ApJ* **680**, 531.
Kumar, P. & Panaitescu, A. (2000). *ApJ* **541**, L51.
Kumar, P., et al. (2007). *MNRAS* **376**, L57.
Lamb, D.Q. (2002). in Lighthouses of the Universe: The Most Luminous Celestial Objects and Their Use for Cosmology, Proc. MPA/ESO, p. 157.
Lamb, D.Q. & Reichart, D.E. (2000). *ApJ* **536**, 1.
Lee, W.H., Ramirez-Riuz, E., & López-Cámara, D. (2007). *ApJ* **699**, L93.
Liang, E., et al. (2008). *ApJ* **675**, 528.
Lyons, N., et al. (2010). *MNRAS* **402**, 705.
MacFadyen, A.I., Ramirez-Ruiz, E., & Zhang, W. (2005). astro-ph/0510192.
Mangano, V., et al. (2007). *A&A* **470**, 105.
Mazets, E., et al. (2008). *ApJ* **680**, 545.
Mazzali, P., et al. (2006). *Nat* **442**, 1018.
Metzger, B.D., Arcones, A., Quataert. E., & Martínez-Pinedo, G. (2010). *MNRAS* **402**, 2771.
Murakami, T. (1991). *Adv. Space Res.* **11**, 119.
Nakar, E., Gal-Yam, A., Piran, T., & Fox, D.B. (2006). *ApJ* **640**, 849.
Norris, J.P. & Bonnell, J.T. (2006). *ApJ* **643**, 266.
Nousek, J.A., et al. (2006). *ApJ* **642**, 389.
Oates, S.R., et al. (2009). *MNRAS* **395**, 490.
O'Brien, P.T., et al. (2006a). *ApJ* **647**, 1213.
O'Brien, P.T., et al. (2006b). *New J. Phys.* **8**, 121.

Palmer, D.M., et al. (2005). *Nat* **434**, 1107.
Panaitescu, A., Mészáros, P., Burrows, D., Nousek, J., Gehrels, N., O'Brien, P., & Willingale, R. (2006). *MNRAS* **369**, 2059.
Peng, F., Königl, A. & Granot, J. (2005). *ApJ* **626**, 966.
Perna, R., Armitage, P.J., & Zhang, B. (2006). *ApJ* **636**, L29.
Pian, E., et al. (2006). *Nat* **442**, 1011.
Piro, L., et al. (1999). *ApJ* **514**, L73.
Piro, L., et al. (2000). *Science* **290**, 955.
Racusin, J., et al. (2008). *Nat* **455**, 183.
Racusin, J.L., et al. (2009). *ApJ* **698**, 43.
Rees, M.J. & Mészáros, P. (1998). *ApJ* **496**, L1.
Reeves, J.N., et al. (2002). *Nat* **416**, 512.
Roming, P.W.A., et al. (2005). *Space Sci. Rev.* **120**, 95.
Roming, P.W.A., et al. (2006). *ApJ* **652**, 1416.
Rosswog, S. (2007). in Triggering Relativistic Jets, ed. W. H. Lee & E. Ramirez-Ruiz, *Rev. Mexicana Astron. Astrof.* , **27**, 57.
Rowlinson, A., et al. (2010). *MNRAS* **409**, 531.
Ruiz-Velasco, A., et al. (2007). *ApJ* **669**, 1.
Rykoff, E.S., et al. (2006). *ApJ* **638**, L5.
Salvaterra, R., et al. (2009). *Nat* **461**, 1258.
Sato, M., Harrison, F.A., & Rutledge, R.E. (2005). *ApJ* **623**, 973.
Sato, G., et al. (2007). *ApJ* **657**, 359.
Soderberg, A.M., et al. (2006). *Nat* **442**, 1014.
Starling, R.L.C., et al. (2010). *MNRAS* **submitted** (arXiv:1004.2919).
Tanvir, N., et al. (2009). *Nat* **461**, 1254.
Troja, E., et al. (2007). *ApJ* **665**, 599.
Villasenor, J.S., et al. (2005). *Nat* **437**, 855.
Watson, D., et al. (2002). *A&A* **393**, 1.
Watson, D., Reeves, J.N., Hjorth, J., Jakobsson, P., & Pedersen, K. (2003). *ApJ* **595**, L29.
Waxman, E., Mészáros, P., & Campana, S. (2007). *ApJ* **667**, 351.
Willingale, R., et al. (2007). *ApJ* **662**, 1093.
Yoshida, A., Murakami, T., Nishimura, J., Kondo, I., & Fenimore, E.E. (1991). *PASJ* **43**, L69.
Yoshida, A., Namiki, M., Otani, C., Kawai, N., Murakami, T., Ueda, Y., Shibata, R., & Uno, S. (1999). *A&A* **138**, 433.
Zhang, B., et al. (2006). *ApJ* **642**, 354.
Zhang, B., Zhang, B.-B., Liang, E.-W., Gehrels, N., Burrows, D.N., & Mészáros, P. (2007). *ApJ* **655**, L25.
Zhang, B., et al. (2009). *ApJ* **703**, 1696.